Energies **2015**, *8*, 1042-1057; doi:10.3390/en8021042

OPEN ACCESS

energies

ISSN 1996-1073

www.mdpi.com/journal/energies

Article

Thermal Model of a Dish Stirling Cavity-Receiver

Rubén Gil *, Carlos Monné, Nuria Bernal, Mariano Muñoz and Francisco Moreno

Mechanical Engineering Department, Engineering and Architecture School, University of Zaragoza; Maria de Luna s/n, Betancourt Building, 50018 Zaragoza, Spain; E-Mails: cmmb@unizar.es (C.M.); nbernal@unizar.es (N.B.); mmunoz@unizar.es (M.M.); fmoreno@unizar.es (F.M.)

* Author to whom correspondence should be addressed; E-Mail: rubengil@unizar.es; Tel.: +34-976-762-188 (ext. 842188).

Academic Editor: Enrico Sciubba

Received: 8 September 2014 / Accepted: 26 January 2015 / Published: 30 January 2015

Abstract: This paper presents a thermal model for a dish Stirling cavity based on the finite differences method. This model is a theoretical tool to optimize the cavity in terms of thermal efficiency. One of the main outcomes of this work is the evaluation of radiative exchange using the radiosity method; for that purpose, the view factors of all surfaces involved have been accurately calculated. Moreover, this model enables the variation of the cavity and receiver dimensions and the materials to determine the optimal cavity design. The tool has been used to study the cavity optimization regarding geometry parameters and material properties. Receiver absorptivity has been identified as the most influential property of the materials. The optimal aperture height depends on the minimum focal space.

Keywords: dish Stirling system; solar cavity-receiver; thermal model; finite difference method; radiosity method; view factors

1. Introduction

The purpose of a dish Stirling cavity to absorb thermal energy from the concentrator and transfer it to the working fluid in the Stirling engine. The power flow through this part of the system is extremely high (concentration ratios in a parabolic dish can be up to 13,000 suns). Therefore, any loss in this part may make the difference between a profitable or unprofitable system. The environmental evaluation of Dish-Stirling made by Bravo *et al.* [1] showed that the dish Stirling technology impact is similar to

photovoltaic facilities. There are several technologies affecting the receiver operation, some of them regarding the system hybridization; Monné *et al.* [2] demonstrated that hybridization showed a clear benefit depending on the fuel used, and Bravo *et al.* [3] studied the environmental impact factor on the receiver depending on the fuel used. In this context, it is necessary to develop a tool to study the cavity performance as a function of its geometry. This will impact the system feasibility.

Several thermal models for dish Stirling cavity receivers have been developed. They analyse the system radiation, convection and conduction losses to determine the efficiency of the designed cavity. These models are usually based on fixed geometries, and some of them, such as those developed by Hogan [4] or Diver [5] consider the AEETES thermal performance numerical model, obtaining results aligned to test data with deviations of 4.1%.

It is not claimed that this study is an exact prediction of real situations; rather the aim of this work is to present a sensitivity analysis by developing a thermal model accurately considering a variable geometry cavity (as an approximate model due to the solar flux distribution considered) and programming view factors.

Regarding radiation losses, some authors have used ray tracing methods (using an algorithm based on the MonteCarlo statistical method) to model the radiative heat transfer. Shuai *et al.* [6] used the MonteCarlo ray-tracing method to predict radiation performance of dish solar concentrator/cavity receiver systems; Li *et al.* [7] studied the radiation flux distributions on the concentrator-receiver system; Müller *et al.* [8] modeled a chemical reactor for thermal dissociation of ZnO using this method, and Nadal *et al.* [9] considered ray-tracing methods to analyse FMSC (Fixed Mirror Solar Concentrator) concentrators for thermal power plants. The main disadvantages of this approach are the long computation times required and the fact that the cavity dimensions are fixed. Another possibility to solve these issues is using the radiosity method, a good approach to deal with semi-gray radiation problems in enclosures. This method was applied by Nepveu *et al.* [10] to obtain a thermal model of a dish Stirling for a cavity divided into 11 different control-volumes. The radiosity method was also used by Gonzalez *et al.* [11] in a numerical study of the heat transfer by natural convection and surface thermal radiation in an open cavity receiver; and Natarajan *et al.* [12] studied the heat transfer in a solar trapezoidal cavity using this method. In 2012, Teichel *et al.* [13] showed an alternative method to calculate the semi-gray radiation heat transfer within an enclosure comprised of diffuse surfaces. In this case, the goal was to obtain a simpler equation system in order to reduce computational time. Moreover, finite volume solutions can be used to solve radiative heat transfer. Martinek *et al.* [14] evaluated the application of this method to a cavity solar receiver by combining finite volume and MonteCarlo methods to reduce the meshing computational load. Deviations from the ideal shape of panels may have an effect on the final performance (Meiser *et al.* [15]), therefore, the modeled solar flux should consider more than these tracing-methods considerations. In order to evaluate convection losses, some researchers have assessed a convective coefficient as a function of different conditions such as internal and external flux, temperature range, receiver inclination and wind velocity. Wu *et al.* [16] reviewed different possible situations in convection losses; concluding that an inclination close to 90° makes the stagnant zone fill the cavity interior space; therefore, a stable temperature stratification is generated, which reduces the convective losses to negligible values. The distribution of this stagnation zone distribution was researched by Prakash *et al.* [17], and the wind influence in that zone was studied by Xiao *et al.* [18], who illustrated the wind velocity, wind inclination, and cavity inclination

influence in the final convection losses. Wu *et al.* [19] studied natural convection heat loss variation, concluding that it is more sensitive to tilt angle and aperture size, except when tilt angle is 90° (when the stagnant zone fills the interior space).

The dish Stirling cavity is a relevant component of the overall system losses. There are no trends or significant results in the available literature to guide a consistent cavity design. This is the main reason for creating a tool to evaluate the variation of this component with geometry and assembly materials.

In this paper, the radiosity method is used to develop a thermal model using EES (Engineering Equation Solver) software [20] and applying the finite difference method. The cavity surface is divided into a variable number of surfaces, depending on the geometry dimensions (which are defined and variable too) and a precision index allowing the user to increase the discretization nodes to apply the finite difference method. View factors are accurately calculated using the reciprocity rule, the sum rule, and the view factor between two coaxial and parallel dishes. Parameters used to program those view factors are functions of the input dimensions and defined among all the possible different cavity surface combinations (functions of the input variables in this model). Convection is calculated using a convective coefficient and an interior and exterior fluid temperature, whose values are defined in agreement with the literature. This coefficient can be varied to analyse different situations. The solar energy source and the material properties are variable parameters too, and the solar flux distribution is considered non-uniform (similar to real conditions [10]). The main purpose of the present model is to analyse some trends in cavity design optimization (geometry and materials) in terms of its efficiency and coming up with an optimization tool to guide the Stirling cavity design.

2. Methodology

The dish Stirling technology consists of a parabolic reflector that concentrates incident solar energy in the receiver (Figure 1). The receiver is the hot source of a Stirling engine and the cavity enables an efficient heat exchange between concentrator and receiver. The basic cavity geometry is shown in Figure 1 and it is composed of a receiver transferring energy to the Stirling engine working fluid, a cavity zone and a second reconcentration zone (to diminish the spillage losses). In this cavity system, the receiver consists of a directly illuminated plane [21].

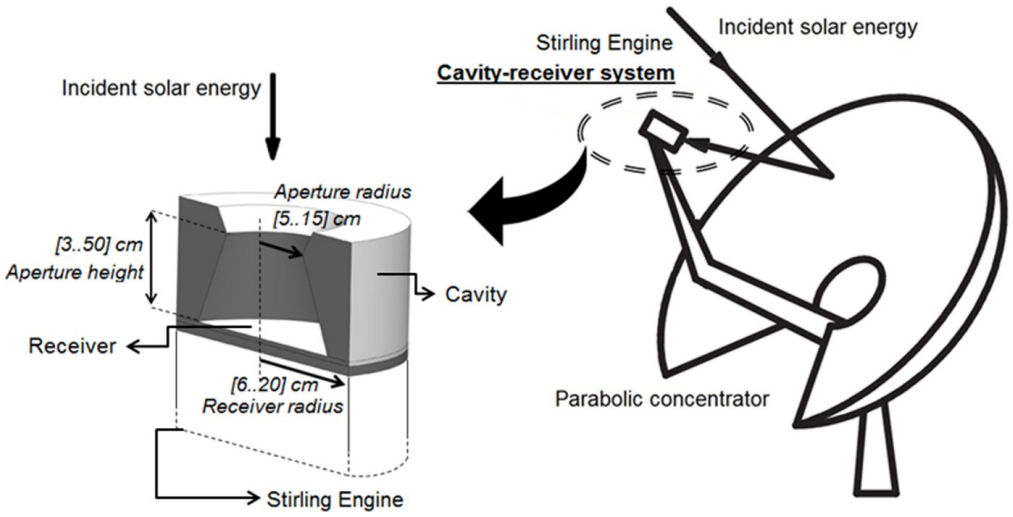

Figure 1. Modeled cavity geometry. Dish Stirling [22].

2.1. Radiation Exchange

The solar energy source is modeled as a non-uniform source. Experimental studies [10] show that the concentrator focuses more energy on the center of the receiver, and hence, the solar flux distribution has been defined setting a central circle and some adjacent crown circles which receive different energy inputs. Axisymmetric distribution has been used in order to simplify calculations.

Radiation exchange is solved considering the electromagnetic radiation spectrum divided in two different bands. One of those bands refers to solar radiation (radiation emitted from the Sun at about 5770 K, $\lambda < 3$ μm), and the other one refers to radiation emission due to the cavity temperature (radiation emitted at about 1000 K, $\lambda < 3$ μm, thermal radiation) [10]. Each one of these two bands is considered an independent phenomenon, and the total effect on the space of study is the sum of both contributions. The surfaces in each one of the different spectra are assumed diffuse and grey.

The solar spectrum can be supposed to only affect the lower part of the volume of the cavity (Figure 2) when the spillage losses are negligible. Each zone represented in Figure 2 presents different concepts. Zone 1 is the plane where the reflected energy leaves the cavity, Zone 2 represents the energy source arriving to the plane and Zone 3 is the cavity lateral surface, divided in a variable number of surfaces. Rings in Zone 2 can be considered different levels of energy of input power.

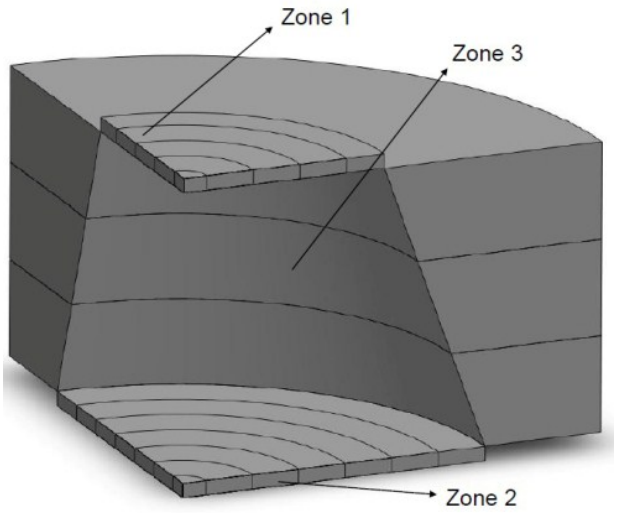

Figure 2. Example surfaces involved in radiation exchange in solar spectrum.

Emission spectrum in thermal radiation affects the entire cavity, and the divisions considered in the lower zone in order to analyse the solar spectrum are completed with those of the upper zone, as shown in Figure 3. Each division is solved as a different surface node temperature. These surfaces are consistent with the finite different discretization and their number and dimensions are functions of the geometry dimension input and the precision variable value.

Figure 3 shows the different analysed zones in thermal radiation. Zone 1 is modeled as a black surface used to connect the two different cavity parts (cavity and reconcentrator). Zone 2 is divided in analogy with the solar spectrum and represents the receiver. Zone 3 represents the cavity lateral surface. Finally, Zone 4 is the environment, modeled as a black surface at environmental temperature.

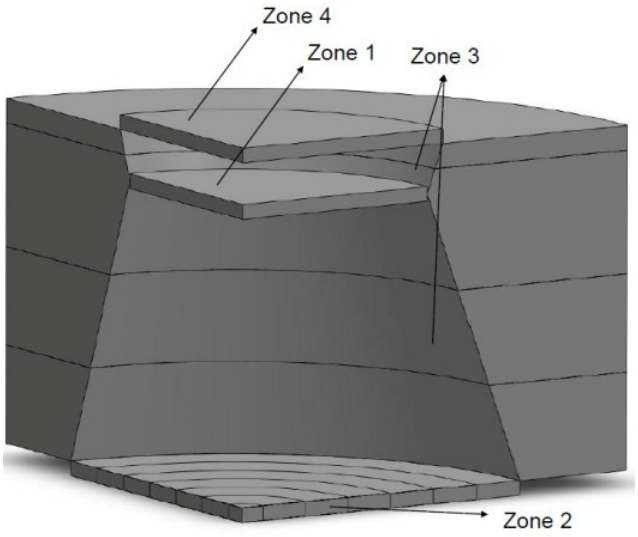

Figure 3. Example surfaces involved in radiation exchange in thermal spectrum.

The following expressions are used to solve the radiation heat exchange among the surfaces involved:

$$q_{i\to j} = A_i \cdot F_{ij} \cdot \left(J_i - J_j\right) \tag{1}$$

$$J_i = J_{es_i} + J_{ec_i} \tag{2}$$

$$J_{ec_i} = \varepsilon\sigma {T_i}^4 + \rho_i \sum_j F_{ij} J_{ec_j} \tag{3}$$

$$J_{es_i} = \rho_i \left(\varphi_i + \sum_j F_{ij} J_{es_j} \right) \tag{4}$$

These previous expressions are used to solve a dynamic mathematical statement (variables and equations quantity change when geometry and precision do). Those equations are obtained considering net radiation heat exchange among surfaces.

2.2. View Factors

In order to evaluate the previous equation system, view factors must be calculated. In this model, it is necessary to create several functions capable of recalculating a different number of view factors depending on the dimensions and the precision variable. This situation requires analysing the discretization and calculation peculiarities. As an example, Figure 4 shows different situations to consider when calculating view factors from a cavity lateral surface.

Each one of the arrows in Figure 4 shows a specific calculation pattern. In order to obtain these view factors a complex calculation process has been carried out based on three basic laws:

- Sum law:

$$\sum_j F_{ij} = 1 \tag{5}$$

- Reciprocity law:

$$A_i F_{ij} = A_j F_{ji} \tag{6}$$

- View factor between two coaxial and parallel dishes [23]:

$$F_{d1d2} = \frac{1}{2}\left\{X - \left[X^2 - 4\left(\frac{x_{d2}}{x_{d1}}\right)^2\right]^{1/2}\right\} \tag{7}$$

$$x_{d1} = \frac{R_{d1}}{\delta} \tag{8}$$

$$x_{d2} = \frac{R_{d2}}{\delta} \tag{9}$$

$$X = 1 + \frac{1 + {x_{d2}}^2}{{x_{d1}}^2} \tag{10}$$

Moreover, the fact that each view factor from one surface to itself is different from 0 (if it is from a lateral surface because of its concave shape) was also considered. The number of surfaces analyzed in the simulated situations in this paper ranges from 50 to 150.

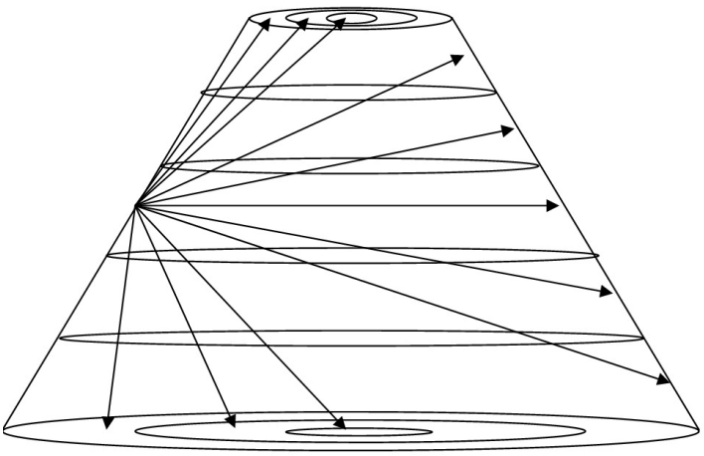

Figure 4. Different view factors calculations from a lateral surface.

2.3. Finite Differences

The thermal modeling in this paper is solved using the finite difference method, formulated for cylindrical control volumes and considering symmetry for resolution. Cavity dimensions are variable and the number of nodes composing the geometry is defined as a function of those variable dimensions and a precision input to change the number of discretization nodes. To apply this method, the expressions to be solved are obtained from an energy balance in each one of the defined nodes [24], so it is necessary to know all heat contributions in the different zones of the cavity to apply their influence in the energy balance. Newton's method extended for solving simultaneous non-linear equations is applied to solve this complex equation system. The relative residuals limit for convergence is fixed to 1e-6, the change in variables limit for convergence is fixed to 1e-9, and the number of iterations is always below 250. While solving, the main numerical results are expressed in Kelvin (temperature), Joules (energy) and centimeters (length).

Heat transfer inside the cavity is due to conduction. When the analysis zone refers to the border of the cavity (contact with Stirling engine, exterior or interior environment), there are not only conduction, but also some other different contributions: convection (contact with exterior "cold" air or interior "hot" air) and radiation (solar spectrum and cavity emission spectrum), as shown in Figure 5. Conduction and convection are solved using Fourier's Law and Newton's Law of Cooling (and Heating).

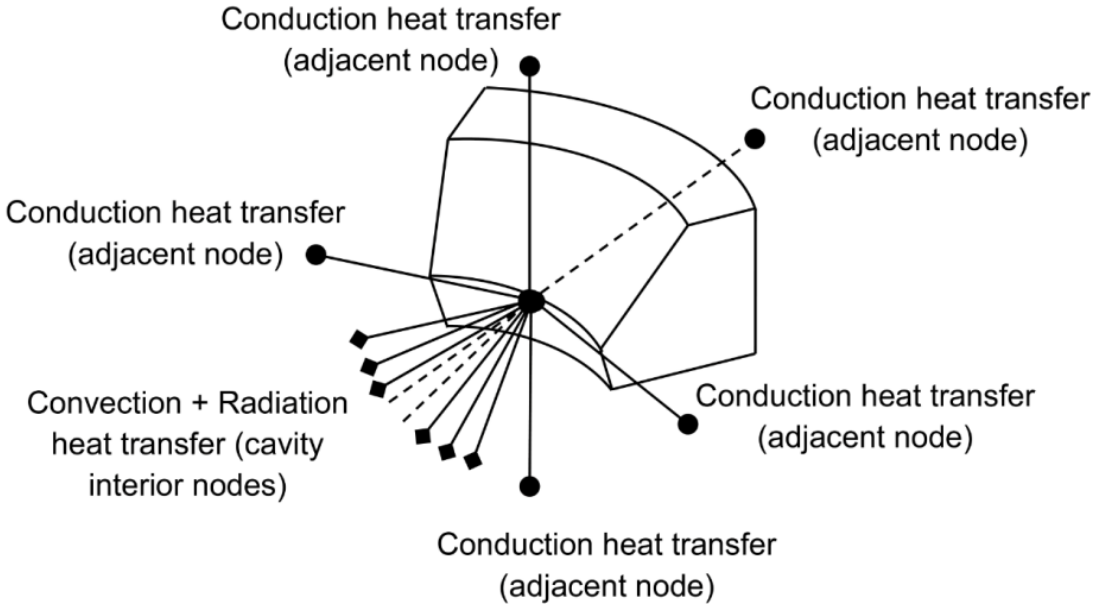

Figure 5. Heat contribution. Cavity border node.

Each one of the analysed nodes presents particular dimensions, and the number of nodes increases when the required precision does. Besides, each node calculation varies from one simulation to another, or from one calculation to another if the dimensions have changed.

3. Cavity Optimization with the EES tool

Using the EES tool proposed in this paper and represented in Figure 6, cavity simulations have been carried out fixing conditions for the parabolic concentrator and the Stirling engine. This paper shows results considering 28 kWt (thermal power) of total energy input, which is the power required to generate approximately 10 kWe (standard electric power of the Cleanergy Stirling engine C11S [25]). Considering these conditions, the geometry and material properties trends for optimization were determined. This optimization was performed in terms of cavity thermal efficiency (η), defined as the ratio between energy transmitted to the engine working fluid and energy received from the concentrator.

Table 1 shows material properties and dimensions in simulations. These values are fixed while not studied for optimization. When aperture radius is studied, reconcentrator radius is considered 3 cm longer than aperture radius, and cavity height is considered 4 cm longer than aperture height (whose value is 9.66 cm). Table 1 shows some parameters values. The same guideline is kept for aperture height and reconcentration radius when aperture height is studied.

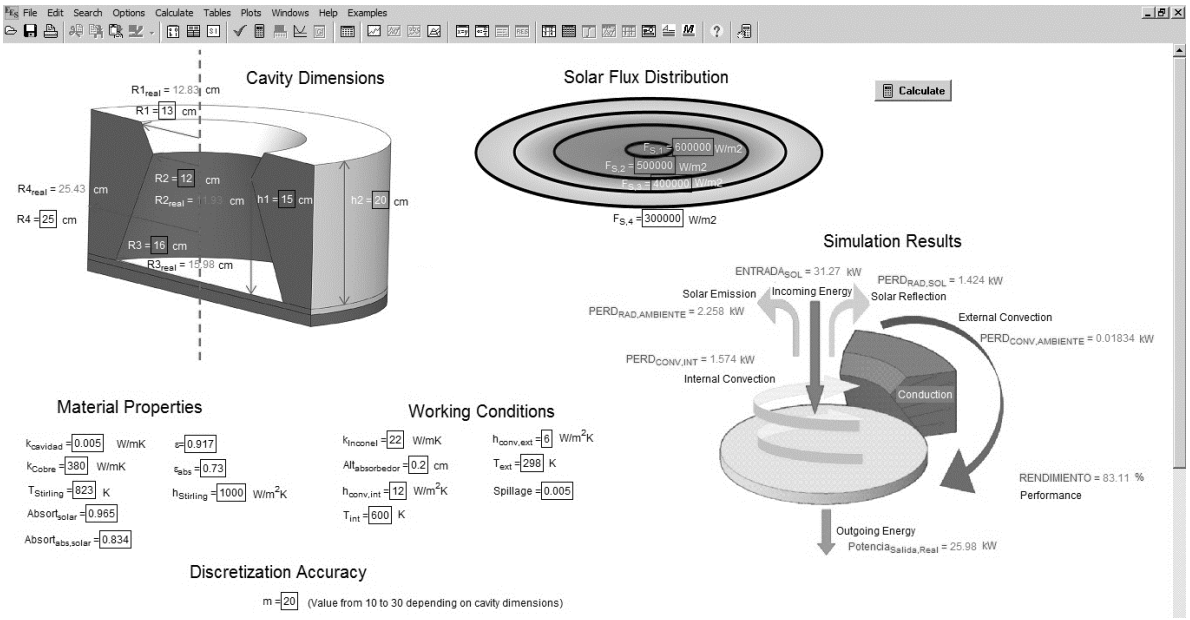

Figure 6. EES (Engineering Equation Solver) tool interface.

Table 1. Material properties and geometrical parameters in simulations.

Material Properties	
Cavity Absorptivity [-]	0.965
Absorber Absorptivity [-]	0.834
Cavity Emissivity [-]	0.917
Absorber Emissivity [-]	0.73
Cavity Conductivity [W/mK]	0.005
Equivalent Convection Coefficient [W/m^{2}K]	6
Equivalent Interior Air Temperature [K]	600
Environment Temperature [K]	298
Geometrical Parameters	
Reconcentrator Radius [cm]	13.28
Aperture Radius [cm]	10.13
Receiver Radius [cm]	15.98
External Cavity Radius [cm]	25.43
Aperture Height [cm]	12.86
Cavity Height [cm]	15

3.1. Finite Differences

One of the goals of this study consists of analysing how different possible dimensions (aperture and height) affect the system efficiency. This objective is reached using the presented thermal model.

Figure 7 shows how the aperture diameter has been varied in this study. The diameter of the cavity base (in contact with the receiver) has been kept constant.

To simulate this situation, the upper cavity zone has been considered fixed. Convection, spillage, radiation, and conduction properties are considered fixed to study this part of the system variation. The aperture diameter affects the efficiency drastically. The trend observed while varying the aperture radius is shown in Figure 8.

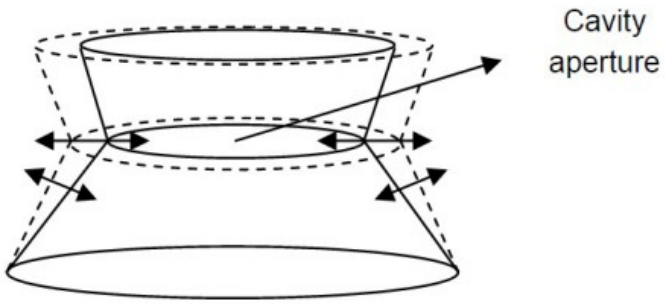

Figure 7. Cavity aperture radius variation.

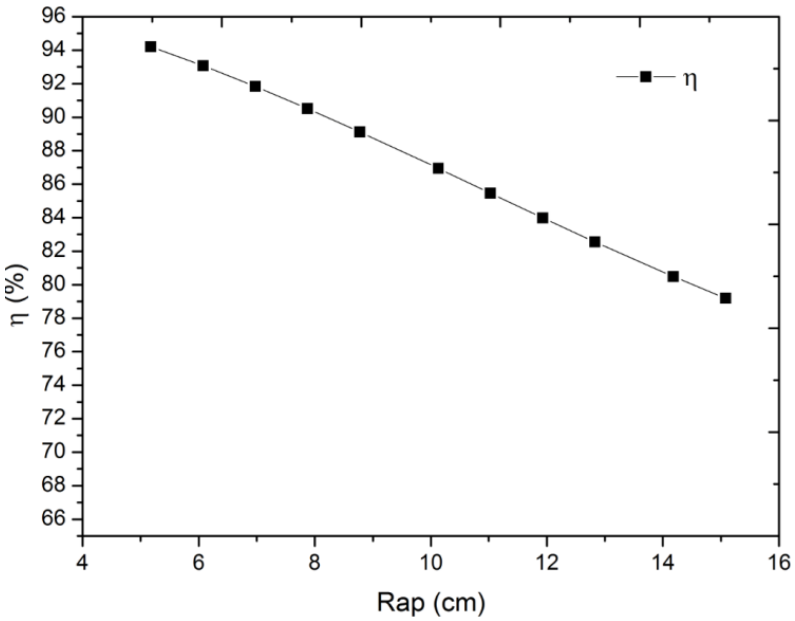

Figure 8. Efficiency against aperture radius (solar source: 28 kWt).

When the aperture radius decreases, the efficiency increases linearly. Emission and reflection losses have been studied too (see Figure 9). Emission losses are greater than reflection ones, and their relative importance depends on the working cavity conditions (because the possible convection losses increase depending on inclination and wind situations [16]).

Once the optimal aperture ratio has been determined, the cavity height influence on efficiency is analysed. Figure 10 shows how the height is varied while keeping the aperture diameter fixed. This analysis sequence has been defined in this way because of the slighter energy efficiency improvement possibility due to height variation (comparing it against aperture ratio variation).

Aperture height influence on efficiency and losses has been studied without any variation in the rest of materials and working conditions parameters. The convection coefficient is varied in this study to consider all possible inclinations and wind conditions. Figure 11 shows how efficiency is modified while varying aperture height when aperture radius reaches 10.13 cm.

The observed behavior in this previous simulation is practically repeated when studying some more radius (Table 2 shows the optimal aperture height for some radius inside the studied range, from 7 to 16 cm).

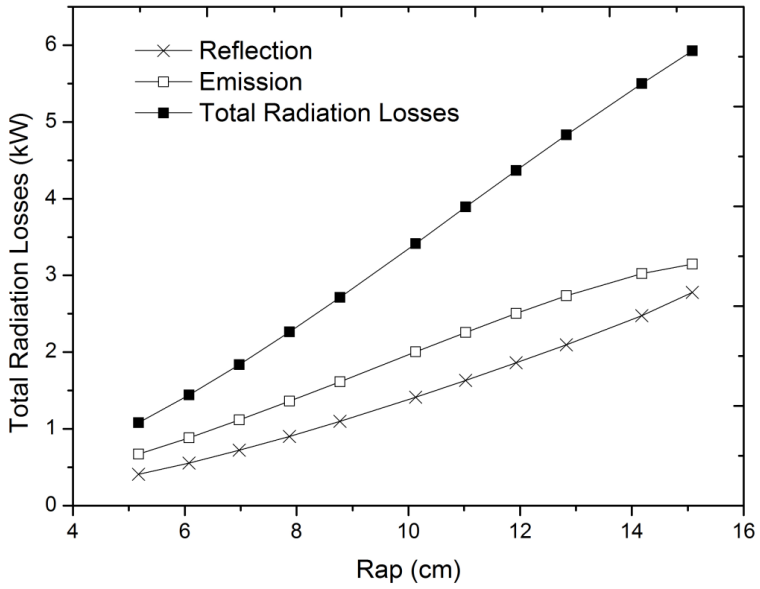

Figure 9. Radiation losses against aperture radius (solar source: 28 kWt).

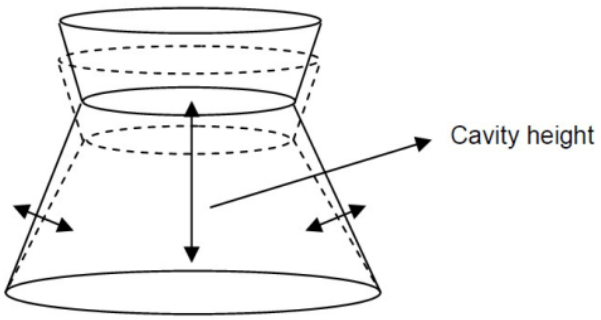

Figure 10. Cavity height variation.

Table 2. Optimal aperture height regarding the studied range for aperture radius.

Aperture Height Analysis	h = 6 W/m^{2}K	h = 12 W/m^{2}K	h = 18 W/m^{2}K	h = 24 W/m^{2}K
Rap = 8 cm	24	9	5	<5
Rap = 10 cm	41	19	13	7
Rap = 12 cm	>45	34	20	12

This reason for this trend is explained as follows: in most of the possible operation cavity conditions and aperture ratio values, efficiency increases up to an optimal height value. If the height increases more than that threshold value, the efficiency decreases. All these variations are relatively soft, and less important than those observed when varying the aperture ratio. That is the reason why aperture ratio should be defined first.

Regarding the remaining cavity dimensions, it can be said that reconcentrator influence on the thermal performance is negligible. Therefore, its design should be directly related to optical considerations. The cavity thickness influence might be relatively important when its value decreases drastically, but there is no limit or condition to set this dimension. The material used is usually based on alumina, a suitable insulator when dealing with radiation and convection losses. In practice, thickness is usually as large as aperture radius, a magnitude that allows considering this influence negligible.

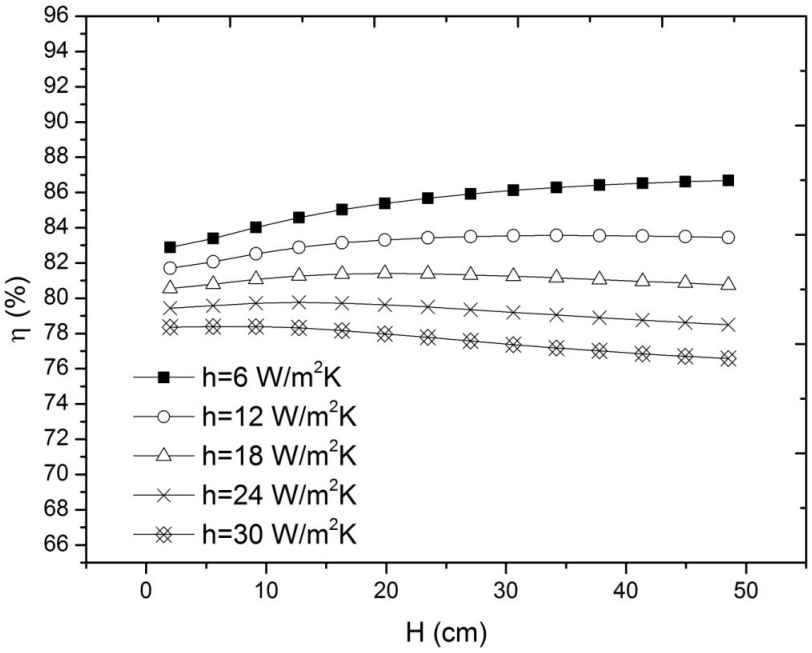

Figure 11. Efficiency varying cavity height (aperture radius = 10.13 cm and receiver radius = 15.98 cm).

3.2. Optimal Material Properties

The present model also enables us to evaluate the influence of material radiant properties. Figures 12 and 13 show the efficiency as a function of absorptivity and emissivity. Each one of the simulations has been carried leaving the rest of variables without any change.

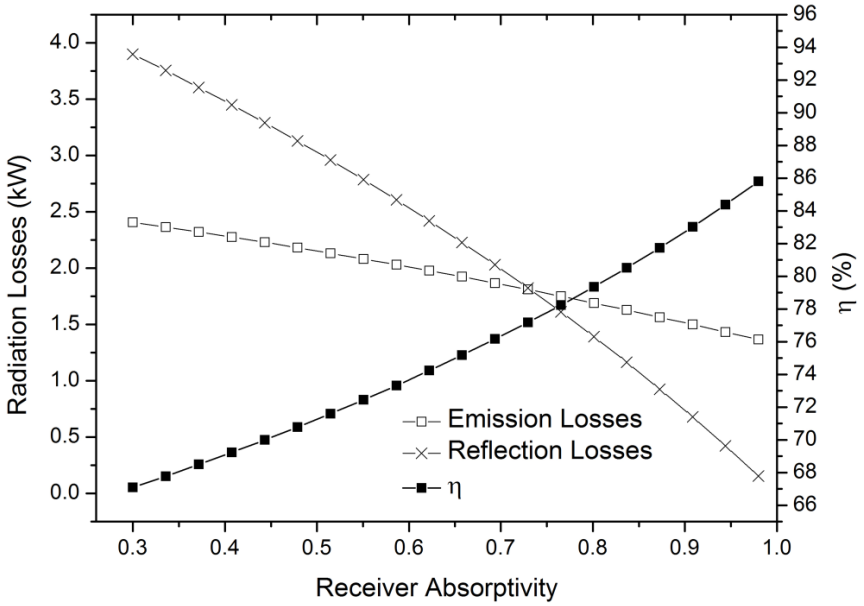

Figure 12. Efficiency and radiation losses varying receiver absorptivity (solar source: 28 kWt).

Receiver absorptivity is the most influential parameter on the system performance. As it is shown in Figure 12, when this parameter increases, radiation losses decrease and the efficiency increase can vary around 20%. The influence of the cavity radiant properties (absorptivity and emissivity) and the

receiver emissivity on the system efficiency is low, as shown in Figures 13 and 14. Figure 13 also shows how emission and reflection losses vary in a compensated way when the cavity absorptivity changes.

Figures 12–14 show how the most important radiation property to vary in order to get more efficiency is the receiver absorptivity. Figure 15 shows the conductivity, whose magnitude can cause the cavity losses to increase from worthless to significant values exponentially. Once the aperture ratio has been chosen knowing the optical concentrator solar properties, cavity height should be determined in order to achieve the optimal performance.

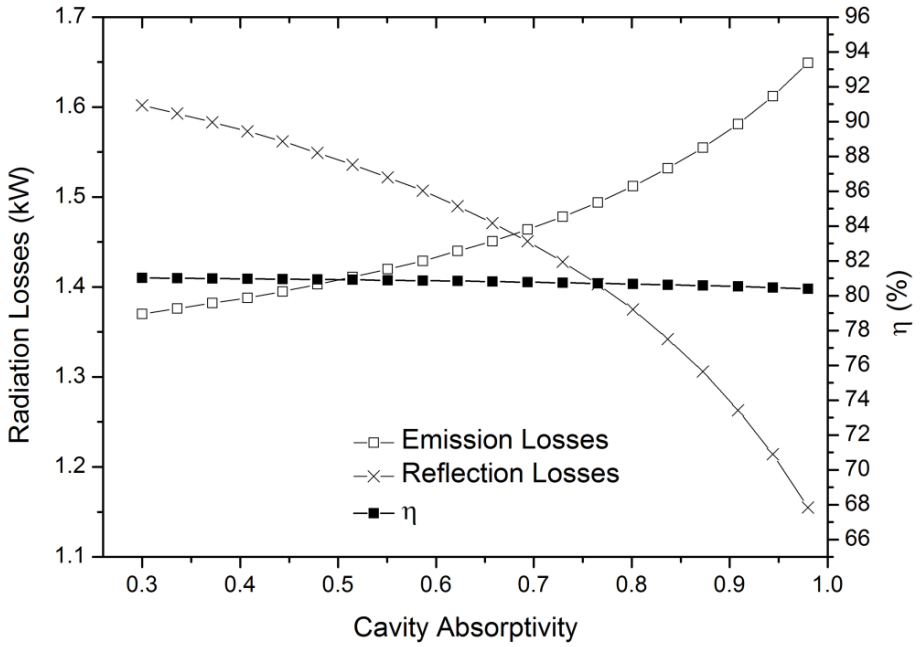

Figure 13. Efficiency and radiation losses varying cavity absorptivity (solar source: 28 kWt).

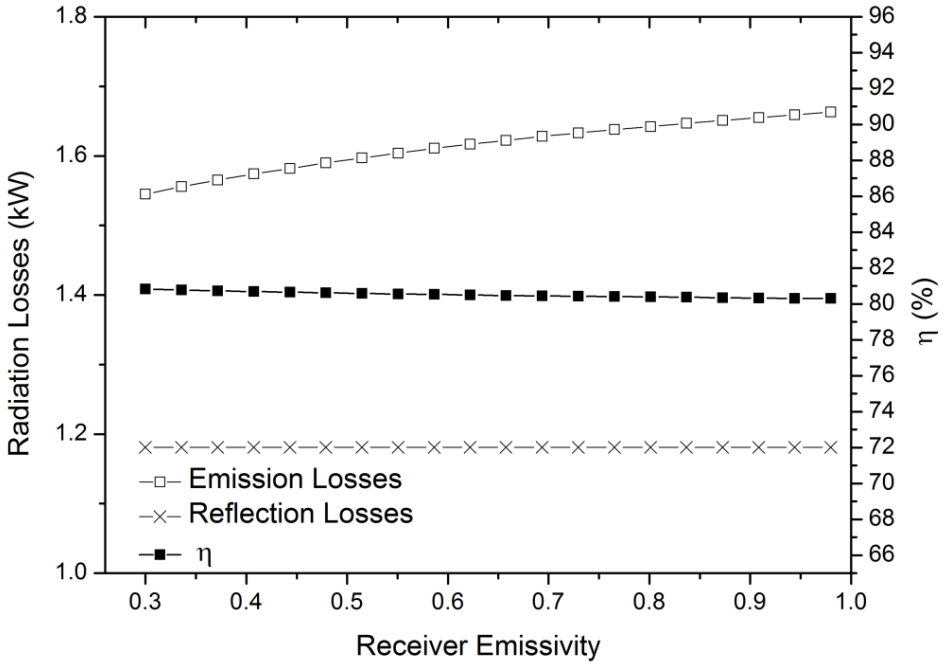

Figure 14. Efficiency and radiation losses varying receiver emissivity (solar source: 28 kWt).

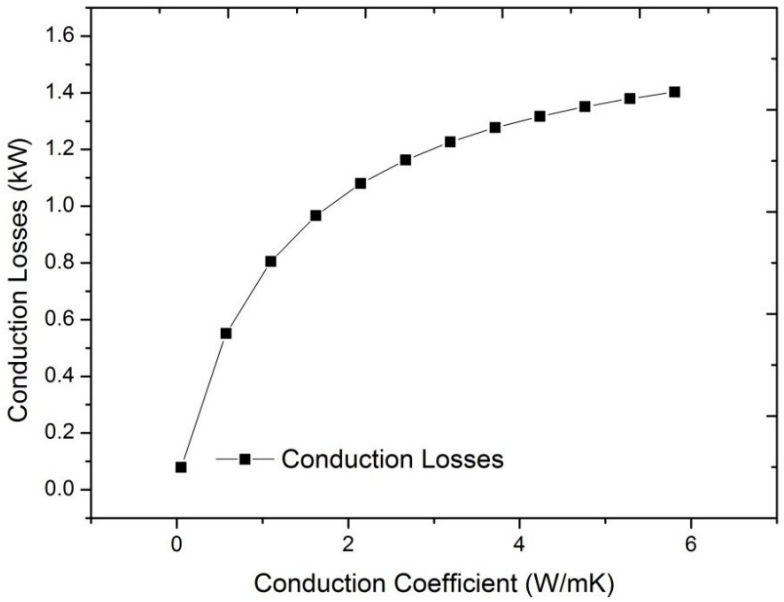

Figure 15. Conduction losses varying conduction coefficient (solar source: 28 kWt).

4. Conclusions

A thermal model for a dish Stirling cavity has been developed applying the finite difference method, using the radiosity method to evaluate radiation heat exchange, and calculating all necessary view factors accurately. Cavity dimensions can be modified because of the dynamic mathematical statement proposed for numerical resolution of the model. This model has been used to create a design tool to find the patterns of the influence of dimensions and material properties on the cavity heat losses. It is concluded that a short aperture radius and high receiver absorptivity make the cavity become much more efficient, whereas cavity height shows an optimal value depending on the aperture ratio (a properly model of flux distribution and spillage influence when varying cavity dimensions determine the first trend about aperture radius). A 28 kWt dish Stirling whose minimal focal space is 12 cm (aperture radius) can achieve a maximum thermal efficiency varying from 79% to 89%, depending on convection conditions. This maximum efficiency is reached when the aperture height of the cavity is near to 20 cm.

This thermal model comes from the growing need to create a design instrument to quantify and evaluate all thermal losses. It is useful to guide the cavity design (dimensions and materials). Once the concentrator has been selected or calculated, and its optical characteristics are known, this tool can be used to obtain the best possible cavity design in terms of thermal efficiency (mainly regarding material properties and the founded trends about geometry optimization). Regarding future works, some cavities designed using this tool will be used for further development and experimental validation.

Acknowledgments

The authors thank the Ministry of Economy and Competitiveness of Spain, for supporting investigation within the project DisHyb "Development of Dish-Stirling cavity-receiver hybrid systems" (Programa Estatal de Investigación, Desarrollo e Innovación Orientada a los Retos de la Sociedad—Plan Estatal de Investigación Científica y Técnica y de Innovación).

Author Contributions

Rubén Gil conceived and programmed the model; Carlos Monné and Nuria Bernal reviewed the model and analysed the data; Mariano Muñoz and Francisco Moreno analysed the data.

Nomenclature

A	Area
F	View factor
H	Aperture cavity height
J	Radiosity
q	Heat transfer
R	Radius
T	Temperature
x	Ratio between dish radius and distance between dishes
X	Coefficient to solve view factor between two coaxial and parallel dishes

Greek symbols

δ	Distance between dish 1 and dish 2
ε	Emissivity
η	Efficiency
λ	Wavelength
ρ	Reflectivity
σ	Stefan-Boltzmann constant (=5.670373 × 10^{-8} W·m^{-2}·K^{-4})
φ	Incident solar flux

Subscripts

ap	Aperture
d1	Dish 1 (view factor calculation)
d2	Dish 2 (view factor calculation)
ec	Emission spectrum (thermal radiation)
i	Surface "i"
j	Surface "j"

Units

cm	Centimeters
K	Kelvin
kW	Kilowatts
kWt	Thermal Kilowatts
m	Meters
m^2	Square meters
W	Watts
μm	Micrometer

Conflicts of Interest

The authors declare no conflict of interest.

References

1. Bravo, Y.; Carvalho, M.; Serra, L.M.; Monné, C.; Alonso, S.; Moreno, F.; Muñoz, M. Environmental evaluation of dish-Stirling technology for power generation. *Sol. Energy* **2012**, *86*, 2811–2825.
2. Monné, C.; Bravo, Y.; Moreno, F. Analysis of a solar dish-Stirling system with hybridization and thermal storage. *Int. J. Energy Environ. Eng.* **2014**, *5*, 1–5.
3. Bravo, Y.; Monné, C.; Bernal, N.; Carvalho, M.; Moreno, F.; Muñoz, M. Hybridization of solar dish-stirling technology: Analysis and design. *Environ. Prog. Sustain. Energy* **2014**, *33*, 1459–1466.
4. Hogan, R.E., Jr. AEETES—A solar reflux receiver thermal performance numerical model. *Sol. Energy* **1994**, *52*, 167–178.
5. Diver, R.B. Reflux solar receiver design considerations. In Proceedings of ASME-JSES-KSES International Solar Energy Conference, Maui, HI, USA, 4–8 April 1992.
6. Shuai, Y.; Xia, X.-L.; Tan, H.-P. Radiation performance of dish solar concentrator/cavity receiver systems. *Sol. Energy* **2008**, *82*, 13–21.
7. Li, Z.; Tang, D.; Du, J.; Li, T. Study on the radiation flux and temperature distributions of the concentrator-receiver system in a solar dish/Stirling power facility. *Appl. Therm. Eng.* **2011**, *31*, 1780–1789.
8. Müller, R.; Steinfeld, A. Band-approximated radiative heat transfer analysis of a solar chemical reactor for the thermal dissociation of zinc oxide. *Sol. Energy* **2007**, *81*, 1285–1294.
9. Nadal, R.P.; Moll, V.M. Optical analysis of the fixed mirror solar concentrator by forward ray-tracing procedure. *J. Sol. Energy Eng.* **2012**, *134*, doi:10.1115/1.4006575.
10. Nepveu, F.; Ferriere, A.; Bataille, F. Thermal model of a dish/Stirling systems. *Sol. Energy* **2009**, *83*, 81–89.
11. Montiel Gonzalez, M.; Hinojosa Palafox, J.; Estrada, C.A. Numerical study of heat transfer by natural convection and surface thermal radiation in an open cavity receiver. *Sol. Energy* **2012**, *86*, 1118–1128.
12. Natarajan, S.K.; Reddy, K.S.; Mallick, T.K. Heat loss characteristics of trapezoidal cavity receiver for solar linear concentrating system. *Appl. Energy* **2012**, *93*, 523–531.
13. Teichel, S.H.; Feierabend, L.; Klein, S.A.; Reindl, D.T. An alternative method for calculation of semi-gray radiation heat transfer in solar central cavity receivers. *Sol. Energy* **2012**, *86*, 1899–1909.
14. Martinek, J.; Weimer, A.W. Evaluation of finite volume solutions for radiative heat transfer in a closed cavity solar receiver for high temperature solar thermal processes. *Int. J. Heat Mass Transf.* **2013**, *58*, 585–596.
15. Meiser, S.; Kleine-Büning, C.; Uhlig, R.; Lüpfert, E.; Schiricke, B.; Pitz-Paal, R. Finite Element Modeling of Parabolic Trough Mirror Shape in Different Mirror Angles. *J. Sol. Energy Eng.* **2013**, *135*, doi:10.1115/1.4023560.

16. Wu, S.-Y.; Xiao, L.; Cao, Y.; Li, Y.R. Convection heat loss from cavity receiver in parabolic dish solar thermal power system: A review. *Sol. Energy* **2010**, *84*, 1342–1355.
17. Prakash, M.; Kedare, S.B.; Nayak, J.K. Determination of stagnation and convective zones in a solar cavity receiver. *Int. J. Therm. Sci.* **2010**, *49*, 680–691.
18. Xiao, L.; Wu, S.Y.; Li, Y.R. Numerical study on combined free-forced convection heat loss of solar cavity receiver under wind environments. *Int. J. Therm. Sci.* **2012**, *60*, 182–194.
19. Wu, S.Y.; Guo, F.H; Xiao, L. Numerical investigation on combined natural convection and radiation heat losses in one side open cylindrical cavity with constant heat flux. *Int. J. Heat Mass Transf.* **2014**, *71*, 573–584.
20. F-Chart Software. Available online: http://www.fchart.com/ (accessed on 27 January 2015).
21. Abate, S.; Barberi, R.; Desiderio, G.; Lombardo, G. Solar Radiation Heat Absorber for a Stirling Motor. World Patent WO2012/016873 A1, 9 February 2012.
22. Li, Y.; He, Y.; Wang, W. Optimization of solar-powered Stirling heat engine with finite-time thermodynamics. *Renew. Energy* **2011**, *36*, 421–427.
23. Incropera, F.P.; DeWitt, D.P. *Fundamentals of Heat and Mass Transfer*; 4th ed.; John Wiley & Sons: New York, NY, USA, 1996; pp. 633–783.
24. Mills, A.F. *Transferencia de Calor*; Irwin: Madrid, Spain, 1995; pp. 129–254. (In Spanish)
25. Cleanergy. Available online: http://www.cleanergy.com (accessed on 5 June 2014).